

# Photoswitchable Organic Nanoparticles and a Polymer Film Employing Multifunctional Molecules with Enhanced Fluorescence Emission and Bistable Photochromism\*\*

Seon-Jeong Lim, Byeong-Kwan An, Sang Don Jung, Myung-Ae Chung, and Soo Young Park\*

Among the various photon-mode molecular memory systems, bistable photoswitching of fluorescence emission is considered to be a promising signaling mode, not only because the fluorescence signals can be readily and sensitively recognized, but also because the small number of photons required for their excitation induce few side effects to spoil the digitalized signals.<sup>[1–9]</sup> Multifunctional fluorescent (including phosphorescent) molecules combining bistable photochromism with built-in 1,2-bis(hienylethene) (BTE) units have been successfully investigated with the aim of applications in ultrahigh-density optical memory media, and they show, in principle, reversible and bistable photoswitching.<sup>[10–15]</sup> The important challenge still remaining unsolved, however, is the general problem of “concentration quenching” in the fluorescence signal, which certainly restricts the application of these multifunctional photochromic molecules to high-density optical memory systems.<sup>[16]</sup> Herein, we demonstrate an innovative approach to this problem by employing a special class of multifunctional photochromic molecule which shows enhanced fluorescence emission with increasing concentration. It is readily expected that the high storage capability, high sensitivity, and high-contrast on/off signaling ratio are synergetically achieved with this molecule in neat nanoparticles or in a highly loaded polymer film.

Very recently, unconventional fluorescent molecules showing aggregation-induced enhanced emission (AIEE) have been reported by several groups including ours.<sup>[17–19]</sup> Simple-structured 1-cyano-*trans*-1,2-bis-(4'-methylbiphenyl)-ethylene (CN-MBE) is a typical AIEE molecule that fluoresces strongly in the solid state even though it is virtually nonfluorescent in solution.<sup>[19]</sup> The multifunctional fluorescent molecule for photoswitchable memory media **1a** was designed and synthesized by replacing one of the end tolyl groups of CN-MBE with the photochromic BTE moiety. Compound **2a**, the non-AIEE analogue of **1a** which lacks

[\*] S.-J. Lim, B.-K. An, Prof. S. Y. Park  
School of Materials Science and Engineering ENG445  
Seoul National University  
San 56-1, Shillim-dong, Kwanak-ku, Seoul 151-744 (Korea)  
Fax: (+82) 2-886-8331  
E-mail: parksy@plaza.snu.ac.kr  
Dr. S. D. Jung, Dr. M.-A. Chung  
Basic Research Laboratory  
Electronics and Telecommunications Research Institute (ETRI)  
161 Gajeong-dong, Yuseong-gu, Daejeon 305-350 (Korea)

[\*\*] This work was supported in part by CRM-KOSEF and ETRI.



Supporting information for this article is available on the WWW under <http://www.angewandte.org> or from the author.

only the CN group, was also synthesized to properly compare the AIEE effect (see Figure 1 for the chemical structures and the Supporting Information for the synthetic details). Compounds **1a** and **2a** were fully identified by  $^1\text{H}$  NMR spectroscopy, FTIR spectroscopy, MALDI-TOF mass spectrometry, and elemental analysis (analytical data are available in the Supporting Information).

Fluorescent photochromic organic nanoparticles (FPONs) of **1a** were prepared by a reprecipitation method to produce a highly concentrated photon-mode recording medium.<sup>[20]</sup> Quite uniform and size-tuned nanoparticles of **1a** (see the scanning electron microscopy (SEM) photograph in Figure 1e) were obtained; the diameters of FPONs of **1a** were  $40 \pm 10$ ,  $125 \pm 25$ ,  $200 \pm 50$ , and  $275 \pm 75$  nm when prepared from THF/water concentrations of  $2 \times 10^{-5}$ ,  $4 \times 10^{-5}$ ,  $1 \times 10^{-4}$ , and  $2 \times 10^{-4}$  M, respectively (other images are available in the Supporting Information). According to the AIEE principle, FPONs of **1a** showed strongly enhanced fluorescence emission, although they were only weakly fluorescent in a THF solution of the same concentration (ca. 1700 times enhancement, compare (II) with (I) in Fig-

ure 1a). This observation contrasts strikingly with the behavior of conventional analogue **2a**, which shows significant concentration quenching in the nanoparticle (ca. 30 times reduction in fluorescence intensity, compare (VI) with (V) in Figure 1c). Such a totally different fluorescence behavior between **1a** and **2a** (AIEE versus quenching) is most probably related to the different aggregation states in their FPONs. In fact, the UV/Vis absorption spectra shown in Figure 2a,c suggest *J*-type and *H*-type aggregations for **1a** and **2a** FPONs, respectively. The absorption spectra of **1a** FPONs were characteristically red-shifted (Figure 2a) and exhibited Mie light scattering as a result of *J*-type aggregation and nanoparticle formation, respectively. Notably, the absorption maxima of FPONs of **1a** showed a gradual red-shift with increasing nanoparticle size;  $\lambda_{\text{max}}^{\text{soln}} = 360$  nm,  $\lambda_{\text{max}}^{\text{FPONs}} = 371$ – $382$  nm with increasing FPON size of 40–275 nm. Concomitantly, FPONs of **1a** showed strongly enhanced fluorescence emission as shown in Figure 2b ( $\Phi_{\text{F}}^{\text{FPONs}} = 3.2$ – $5.1$  %,  $\lambda_{\text{max}}^{\text{FPONs}} = 485$ – $493$  nm) compared with the isolated **1a** dissolved in THF ( $2 \times 10^{-4}$  M,  $\Phi_{\text{F}}^{\text{soln}} = 0.002$  %,  $\lambda_{\text{max}}^{\text{soln}} = 461$  nm).<sup>[21,22]</sup> All of these spectral changes corroborate that the *J*-type aggregation and

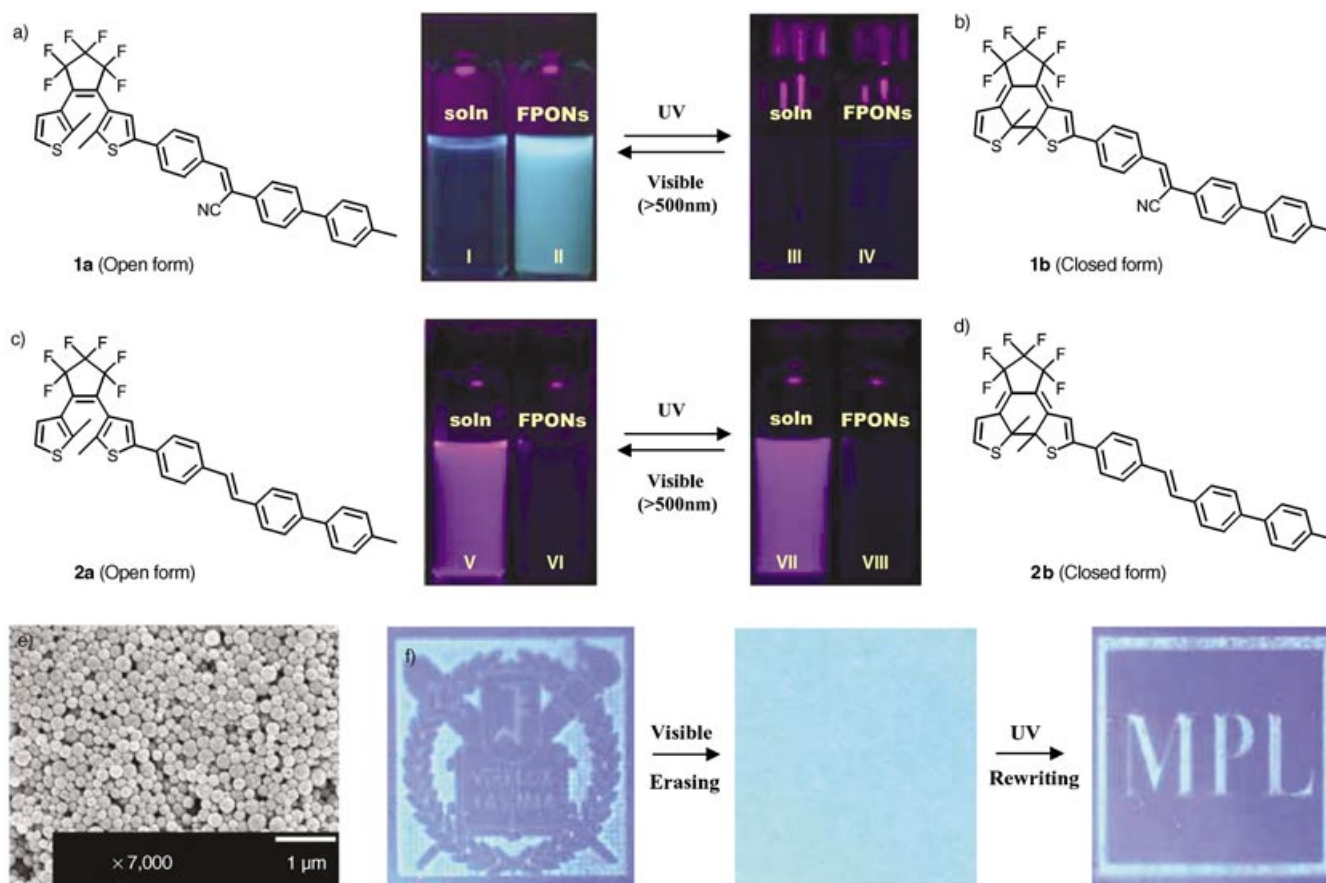


**Figure 1.** a) Chemical structure of **1a** and the fluorescence images of its THF solution (I, soln,  $2 \times 10^{-4}$  M) and the colloidal suspension (II) of fluorescent photochromic organic nanoparticles (FPONs;  $2 \times 10^{-4}$  M). b) Chemical structure of **1b** and the fluorescence images of its THF solution (III,  $2 \times 10^{-4}$  M) and the colloidal suspension of FPONs (IV,  $2 \times 10^{-4}$  M) in the photostationary state (PSS). c) Chemical structure of **2a** and the fluorescence images of its THF solution (V,  $2 \times 10^{-5}$  M) and the colloidal suspension of FPONs (VI,  $2 \times 10^{-5}$  M). d) Chemical structure of **2b** and the fluorescence images of its THF solution (VII,  $2 \times 10^{-5}$  M) and the colloidal suspension of FPONs (VIII,  $2 \times 10^{-5}$  M) in the PSS. e) FE-SEM image of FPONs of **1a** ( $275 \pm 75$  nm) prepared from a THF/water mixture ( $2 \times 10^{-4}$  M). f) Photo-rewritable fluorescence imaging on the polymer film loaded with 20 wt% of **1a** by using UV (365 nm, hand-held lamp,  $1.2 \text{ mWcm}^{-2}$ ) and visible light ( $> 500$  nm). The dark regions represent the parts irradiated with UV light; the real size of the photomasks is about  $1 \text{ cm} \times 1 \text{ cm}$ .

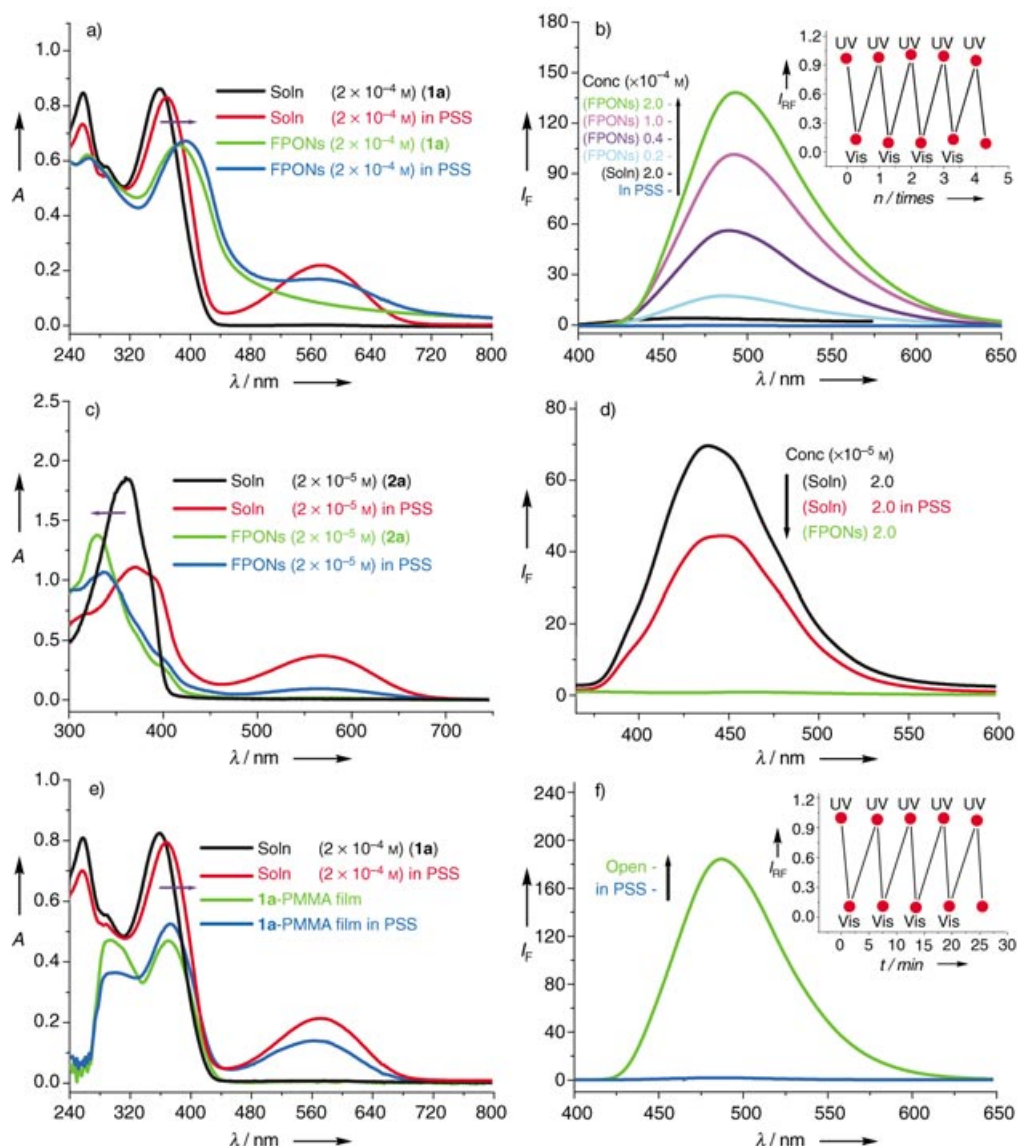


**Figure 2.** a) UV/Vis absorption spectra of **1a** in THF ( $2 \times 10^{-4}$  M) and the colloidal suspension of FPONs of **1a** ( $2 \times 10^{-4}$  M). b) PL spectra of FPONs of **1a** ( $275 \pm 75$  nm) in the PSS (bottom, blue line), **1a** in THF ( $2 \times 10^{-4}$  M, black line), and size-tuned FPONs of **1a** of 40–275 nm (cyan-green line, respectively). The inset graph shows a relative PL intensity modulation of **1a** FPONs ( $275 \pm 75$  nm). c), d) UV/Vis absorption and PL spectra of **2a** in THF ( $2 \times 10^{-5}$  M) and the colloidal suspension of **2a** FPONs ( $2 \times 10^{-5}$  M). e) UV/Vis absorption spectra of **1a** in THF ( $2 \times 10^{-4}$  M) and a 20 wt% **1a**-loaded PMMA film. f) PL spectra of the 20 wt% **1a**-loaded PMMA film. The inset graph shows the relative PL intensity modulation of the film.

molecular planarization of **1a** molecules were induced in their FPONs by specific intermolecular interactions.<sup>[19,23]</sup> In contrast, the UV/Vis absorption spectra of **2a** FPONs were significantly blue-shifted ( $\lambda_{\text{max}}^{\text{soln}} = 360$  nm,  $\lambda_{\text{max}}^{\text{FPONs}} = 329$  nm) as shown in Figure 2c. Moreover, the fluorescence quantum yield of FPONs of **2a** was drastically reduced by 30 times from that of a solution of **2a** in THF ( $2 \times 10^{-5}$  M,  $\Phi_{\text{F}}^{\text{soln}} = 3.4\%$ ,  $\lambda_{\text{max}}^{\text{soln}} = 439$  nm,  $\Phi_{\text{F}}^{\text{FPONs}} = 0.1\%$ ) as indicated in Figure 2d. This blue-shifted UV absorption together with the salient concentration quenching in FPONs of **2a** is attributed to the formation of *H*-type aggregation through strong cofacial  $\pi$ -stacking interactions, which most likely provides a nonradiative decay route.<sup>[24,25]</sup>

Compounds **1a** and **2a** with open-ring BTE units were converted into **1b** and **2b** with closed-ring BTE units when irradiated with UV light ( $365$  nm,  $1.2$  mW cm<sup>-2</sup>). This process was easily monitored by the appearance of new absorption bands in the visible regions ( $\lambda_{\text{max}}^{\text{1b}} = 574$  nm,  $\lambda_{\text{max}}^{\text{2b}} = 570$  nm) as shown in Figure 2a,c (see the Supporting Information for details). Accompanied by this photochromic ring closure, the photoluminescence (PL) intensities of the **1a** FPONs were greatly reduced (compare (IV) with (II) in Figure 1a,b, and see the Supporting Information for details). The fluorescence quantum yields of the FPONs of **1a** in the photostationary state (PSS)<sup>[15]</sup> were reduced by 16–170 times ( $\Phi_{\text{F}}^{\text{FPONs}} = 0.20, 0.09, 0.04$ , and  $0.02\%$  in the PSS,  $\Phi_{\text{F}}^{\text{FPONs}} = 3.2, 5.1, 4.1$ , and  $3.4\%$  in the **1a** form with increasing FPON size of 40–275 nm,

respectively).<sup>[21,22]</sup> However, only a small amount of fluorescence modulation (29% reduction, see the Supporting Information for details) was achieved in a solution of **2a** ( $2 \times 10^{-5}$  M,  $\Phi_F^{\text{soln}} = 2.4\%$  in the PSS,  $\Phi_F^{\text{soln}} = 3.4\%$  in the **2a** form).

It is known that there are two interconvertible conformations of BTE units: one is a parallel conformation and the other is an antiparallel conformation, of which only the latter allows an electrocyclic ring-closing reaction.<sup>[15]</sup> Through the <sup>1</sup>H NMR spectroscopic study ( $2 \times 10^{-4}$  M of CDCl<sub>3</sub> solution, 22 °C, 300 MHz) it was determined that the parallel and antiparallel conformations of **1a** were equally populated, and also that only about 35% of the **1a** forms were photoisomerized to the **1b** forms in the PSS under irradiation with 365 nm light.<sup>[26,27]</sup> An even smaller extent of ring-closing reaction in the PSS is implied for FPONs of **1a**, because the net absorbance of the **1b** form at 574 nm is smaller in FPONs than in solution (see Figure 2a). It is reasonably supposed, therefore, that the photochromic interconversion between the two conformations was suppressed within a FPON (which is essentially a condensed solid state), or that the ring-closing reactions occurred only at the surfaces of the FPONs.<sup>[28]</sup> Given that the extent of the ring-closing reaction is less than 35%, the experimentally observed extremely large reduction in the fluorescence quantum yield  $\Phi_F$  (16–170-fold decrease) of FPONs of **1a** in the PSS must be achieved not only by intramolecular energy transfer between the fluorophore and the closed-ring form of BTE, although it is very likely that the 29% reduction of the  $\Phi_F$  value of the **2a** solution occurs through this intramolecular energy transfer.<sup>[2–5,7,8]</sup> It is presumed that the condensed-state FPONs also provide an additional quenching event, or intermolecular energy transfer between the unconverted **1a** forms and the neighboring **1b** forms, because of their proximity in FPONs. Consequently, extremely high contrast in the on/off signaling ratio is automatically implemented in the neat FPONs of **1a**, which is an additional advantage to the enhanced fluorescence and high storage capacity of the AIEE molecule.

Moreover, when the FPONs of **1a** in the “off” state were irradiated with visible light (> 500 nm), the PL intensities were perfectly recovered to those of the initial “on” state as a result of the reversible photochromic behavior of the BTE unit. The inset graph in Figure 2b shows a reversible photochromic modulation of relative fluorescence intensity in the suspension of FPONs of **1a** under alternating irradiation with UV and visible light (note the on/off fluorescence intensity ratio > 10).

To produce a more practical photo-rewritable imaging medium we prepared a strongly fluorescent poly(methyl methacrylate) (PMMA;  $M_w = \text{ca. } 120\,000$ ) film containing a very high level (20 wt %,  $\text{ca. } 3 \times 10^{-1}$  M) of **1a** molecules. This polymer film was optically clear and scatter-free, presumably because of the partial miscibility of PMMA and **1a**. The absence of light scattering and detectable aggregate features in the fluorescence-enhanced (FE) SEM image (down to  $\text{ca. } 10$  nm scale, see Supporting Information), which are, however, accompanied by distinct *J*-type red-shifted absorption in the film ( $\lambda_{\text{max}}^{\text{soln}} = 360$  nm,  $\lambda_{\text{max}}^{\text{film}} = 372$  nm, see Figure 2e), suggests that the film comprises molecular-scale aggregates of

**1a**. The presence of molecular-scale aggregates is additionally evidenced by the strong effect of AIEE as the intense blue fluorescence ( $\Phi_F^{\text{film}} = 5.8\%$ ,  $\lambda_{\text{max}}^{\text{film}} = 487$  nm versus  $\Phi_F^{\text{soln}} = 0.002\%$ ,  $\lambda_{\text{max}}^{\text{soln}} = 461$  nm in  $2 \times 10^{-4}$  M solution) from this polymer film (see Figure 2f).<sup>[21,29,30]</sup> The AIEE fluorescence from this PMMA/**1a** film was also photoswitched in a bistable manner by alternate UV and visible light irradiation with high contrast ( $\Phi_F^{\text{film}} = 0.3\%$  in the PSS,  $\Phi_F^{\text{film}} = 5.8\%$  in the **1a** form, or on/off fluorescence intensity ratio > 19), as shown in the inset graph in Figure 2f. In addition, the practical capability of rewritable fluorescence photoimaging on our AIEE polymer film was investigated by patterned illumination through photomasks. The emblem of Seoul National University was recorded as a first image (Figure 1f), which was subsequently erased and followed by the recording of a second image, the abbreviation of the Molecular Photonics Laboratory (MPL). This successful demonstration of rewritable photoimaging on the polymer film suggests immediate application of **1a** molecules to ultrahigh-density rewritable optical memory media or imaging processes.

In conclusion, we designed and synthesized a special class of multifunctional molecule **1a**, which shows a strongly enhanced fluorescence emission as well as bistable photochromism. High-contrast (> 10) on/off fluorescence switching was successfully implemented in the size-tuned neat nanoparticles of **1a** and also in a PMMA film highly loaded with **1a**.

Received: July 3, 2004

**Keywords:** aggregation · fluorescence · nanotechnology · photochromism · polymers

- [1] A. Fernandez, J.-M. Lehn, *Adv. Mater.* **1998**, *10*, 1519–1522.
- [2] T. Kawai, T. Sasaki, M. Irie, *Chem. Commun.* **2001**, 711–712.
- [3] K. Yagi, C. F. Soong, M. Irie, *J. Org. Chem.* **2001**, *66*, 5419–5423.
- [4] A. Osuka, D. Fujikane, H. Shinmori, S. Kobatake, M. Irie, *J. Org. Chem.* **2001**, *66*, 3913–3923.
- [5] T. B. Norsten, N. R. Branda, *J. Am. Chem. Soc.* **2001**, *123*, 1784–1785.
- [6] B. Chen, M. Wang, Y. Wu, H. Tian, *Chem. Commun.* **2002**, 1060–1061.
- [7] T. Kawai, M.-S. Kim, T. Sasaki, M. Irie, *Opt. Mater.* **2002**, *21*, 275–278.
- [8] M. Irie, T. Fukaminato, T. Sasaki, N. Tamai, T. Kawai, *Nature* **2002**, *420*, 759–760.
- [9] S. Murase, M. Teramoto, H. Furukawa, Y. Miyashita, K. Horie, *Macromolecules* **2003**, *36*, 964–966.
- [10] M. Irie, *Photoreactive Materials for Ultrahigh-Density Optical Memory*, Elsevier, Amsterdam, **1994**.
- [11] J. C. Crano, R. J. Guglielmetti, *Organic Photochromic and Thermochromic Compounds, Vol. 1*, Plenum, New York, **1999**.
- [12] S. Nakamura, M. Irie, *J. Org. Chem.* **1988**, *53*, 6136–6138.
- [13] Y. Nakayama, K. Hayashi, M. Irie, *J. Org. Chem.* **1990**, *55*, 2592–2596.
- [14] M. Hanazawa, R. Sumiya, Y. Horikawa, M. Irie, *J. Chem. Soc. Chem. Commun.* **1992**, 206–207.
- [15] M. Irie, *Chem. Rev.* **2000**, *100*, 1685–1716.
- [16] J. B. Birks in *Photophysics of Aromatic Molecules*, Wiley, London, **1970**.

- [17] J. Luo, Z. Xie, J. W. Y. Lam, L. Cheng, H. Chen, C. Qiu, H. S. Kwok, X. Zhan, Y. Liu, D. Zhu, B. Z. Tang, *Chem. Commun.* **2001**, 1740–1741.
- [18] H. Murata, Z. H. Kafafi, M. Uchida, *Appl. Phys. Lett.* **2002**, 80, 189–191.
- [19] B. K. An, S. K. Kwon, S. D. Jung, S. Y. Park, *J. Am. Chem. Soc.* **2002**, 124, 14410–14415.
- [20] Preparation of FPONs: All suspensions of FPONs were prepared by the reprecipitation method from THF solution with distilled water. Volume fractions of THF and water were adjusted to 20 and 80 %, respectively. See ref. [19] for details.
- [21] Fluorescence quantum yields: The fluorescence quantum yields ( $\Phi_F$ ) were relatively calculated using 9,10-diphenylanthracene (DPA) in benzene (see ref. [22]) and in PMMA (see refs. [29,30]) as a standard reference ( $1 \times 10^{-3}$  M,  $\Phi_F = 83$  %). Through this method, the  $\Phi_F$  values of FPONs of **1a** were determined as 3.2, 5.1, 4.1, and 3.4 % ( $\lambda_{\text{max em}}^{\text{FPONs}} = 485, 489, 491, \text{ and } 493 \text{ nm}$ ,  $\lambda_{\text{max abs}}^{\text{FPONs}} = 371, 374, 378, \text{ and } 382 \text{ nm}$ ) in the **1a** form, and as 0.20, 0.09, 0.04, and 0.02 % in the PSS with increasing FPON size of  $40 \pm 10$ ,  $125 \pm 25$ ,  $200 \pm 50$ , and  $275 \pm 75 \text{ nm}$ , respectively. It is reasonably considered that the slight reduction of the  $\Phi_F$  values in  $200 \pm 50$  and  $275 \pm 75 \text{ nm}$  FPONs of **1a** results from the highly increased virtual absorbance values by increased light scattering. In fact, the extent of the apparent absorbance of the FPONs of **1a** at the excitation wavelength, that is at 360 nm, was almost linearly proportional to their suspension concentrations in spite of the inverse proportional relationship between the mean radius and the surface-to-volume ratio of the FPONs.
- [22] I. B. Berlman in *Handbook of Fluorescence Spectra of Aromatic Molecules*, Academic Press, New York, **1971**.
- [23] H. Auweter, H. Haberkorn, W. Heckmann, D. Horn, E. Lüddecke, J. Rieger, H. Weiss, *Angew. Chem.* **1999**, 111, 2325–2328; *Angew. Chem. Int. Ed.* **1999**, 38, 2188–2191.
- [24] A. V. Ruban, P. Horton, A. J. Young, *J. Photochem. Photobiol. B* **1993**, 21, 229–234.
- [25] L. Dahne, E. Biller, *Adv. Mater.* **1998**, 10, 241–245.
- [26] Determination of the conformational population and conversion rate: A  $^1\text{H}$  NMR spectroscopic study ( $2 \times 10^{-4}$  M of  $\text{CDCl}_3$  solution,  $22^\circ\text{C}$ , 300 MHz) on the **1a** form showed that the parallel and antiparallel conformations were equally populated in solution, as evident by there only being two singlet resonances at  $\delta = 1.98$  and  $1.91 \text{ ppm}$  without any splitting. These signals were assigned as the methyl protons at the 2-positions of the thiophene rings of the **1a** form (see ref. [27]). The conversion rate of about 35 % in the PSS was calculated by the integrated ratio between the singlet peaks of methyl protons in the **1a** form and those in the **1b** form, which newly appeared at  $\delta = 2.15$  and  $2.11 \text{ ppm}$ .
- [27] M. Irie, K. Sakemura, M. Okinaka, K. Uchida, *J. Org. Chem.* **1995**, 60, 8305–8309.
- [28] F. Sun, F. Zhang, F. Zhao, X. Zhou, S. Pu, *Chem. Phys. Lett.* **2003**, 380, 206–212.
- [29] G. G. Guilbault, *Practical Fluorescence*, Marcel Dekker, New York, **1990**.
- [30] X. Zhang, A. S. Shetty, S. A. Jenekhe, *Macromolecules* **1999**, 32, 7422–7429.